

# Who Checks the Checker?

## Enhancing Component-level Architectural SEU Fault Tolerance for End-to-End SoC Protection

Michael Rogenmoser\*<sup>✉</sup>, Philippe Sauter\*<sup>✉</sup>, Chen Wu\*<sup>✉</sup>, Angelo Garofalo\*<sup>†</sup><sup>✉</sup>, Luca Benini\*<sup>†</sup><sup>✉</sup>

\*ETH Zürich, Zürich, Switzerland

†University of Bologna, Bologna, Italy

**Abstract**—Single-event upset (SEU) fault tolerance for systems-on-chip (SoCs) in radiation-heavy environments is often addressed by architectural fault-tolerance approaches protecting individual SoC components (e.g., cores, memories) in isolation. However, the protection of voting logic and interconnections among components is also critical, as these become single points of failure in the design. We investigate combining multiple fault-tolerance approaches targeting individual SoC components, including interconnect and voting logic to ensure end-to-end SoC-level architectural SEU fault tolerance, while minimizing implementation area overheads. Enforcing an overlap between the protection methods ensures hardening of the whole design without gaps, while curtailing overheads. We demonstrate our approach on a RISC-V microcontroller SoC. SEU fault-tolerance is assessed with simulation-based fault injection. Overheads are assessed with full physical implementation. Tolerance to over 99.9% of faults in both RTL and implemented netlist is demonstrated. Furthermore, the design exhibits 22% lower implementation overhead compared to a single global fault-tolerance method, such as fine-grained triplication.

### I. INTRODUCTION

Fault tolerance of integrated circuits and systems-on-chip (SoCs) is of crucial importance for systems operating in radiation-heavy or safety-critical environments. Space [1], high-energy physics detectors [2], avionics [3], and functional-safety automotive systems [4] increasingly deploy complex safe microcontroller-class SoCs that must continue operating correctly even under single-event upsets (SEUs) and single-event transients (SETs). In many of these domains, even a single undetected or uncorrected error is unacceptable, as silent data corruption can compromise mission objectives, safety guarantees, or system-wide dependability requirements. On the other hand, the area overhead of fault tolerance is always a concern as it implies a significant cost increase.

Commercial designs targeting space applications, such as the NOEL-V SoC [5], often rely on radiation-hardened technologies to achieve fault-tolerance, accompanied by architectural solutions such as error correction codes (ECC). While these technologies can reduce the likelihood of SEUs in the design, they do not prevent them completely. Further, they add area, timing, and power overhead, and are not always available, especially for modern technology nodes.

As an alternative, fault-tolerance can be addressed at the architectural level. Fine-grained triplication of the entire SoC design [2], [6] is a classic approach in high-energy physics, leveraging tools such as Triple Modular Redundancy Generator (TMRG) [7], which triplicates the entire design

and adds voters throughout. While these solutions avoid depending on radiation-hardened technologies, they come at a very high cost, showing a  $4.8 \times$  to  $6.9 \times$  area increase [2] compared to the baseline, unprotected, SoC.

To reduce the area overhead, numerous architectural fault-tolerance approaches have been proposed to protect individual SoC components (e.g., cores, memories) with component-specific approaches. A common technique is lockstepped processor cores execution [8]–[12], which enables error detection at the cores' boundary through checking or voting mechanisms. Other methods [13], [14] protect critical units within the processor cores, in an effort to further decrease overhead with respect to full-core lockstep. Additional work [15] adds triple modular redundancy (TMR) to flip-flops (FFs) in the design, along with dedicated lockstepping of the processor and fault monitors, but still fails to address SETs in combinational logic connecting the TMR FFs. Yet all these approaches introduce a new vulnerability: the voters and checking logic themselves, which remain unprotected. While small in area, these components become critical points of failure. To address this issue, the voters may require an implementation based on radiation-hardened gates and libraries [16]. Unfortunately, such gates and libraries are not always available, especially when targeting advanced technologies.

Furthermore, the combination of component-level architectural fault tolerance techniques is rarely examined in terms of how they interact when applied together to protect an entire SoC. Prior work [17] evaluating a SoC protected with ECC memory and triple-core lockstep (TCLS) processor cores clearly shows that, especially in extreme environments, only applying such techniques is insufficient, as the remaining vulnerable components at the boundaries and outside the protected regions have a significant residual impact on end-to-end SoC-level reliability. The necessity to properly protect peripherals is also highlighted in [18], yet it is often left as a minor concern. These observations strongly motivate the need for end-to-end methods and their evaluation that ensure that all components, including voting, encoding, and interconnect logic, are protected while minimizing area overheads.

To address these challenges, we propose targeted protection methods for each subsystem in a SoC, with a novel *overlapping protection approach*. Overlap, where the checking logic of one domain using method A is included within the connected protection domain using method B, enforces that the boundary logic between protection domains, including voters and ECC decoders/encoders, is never left exposed, ensuring that errors in the checking logic itself are detected and

This work has received funding from the Swiss State Secretariat for Education, Research, and Innovation (SERI) under the SwissChips initiative.

corrected. We demonstrate our approach on `croc`, a compact RISC-V microcontroller unit (MCU) SoC, and show through simulation-based fault injection that overlapping protection defines a new Pareto-optimal point in the reliability–area design space, achieving over 99.9% fault coverage while reducing area by 22% compared to full triplication.

The contributions of the paper are:

- A novel architectural fault-tolerance overlapping method to ensure detection and correction even for the checkers and voters at the boundary of protected components (without resorting to rad-hard gates).
- A complete fault-tolerant RISC-V-based MCU SoC using dedicated architectural fault tolerance methods for each component, and exploiting overlapping protection, to achieve full end-to-end fault-tolerance.
- Analysis of the timing and area impacts of incrementally adding protection methods.
- A comprehensive validation of the proposed architecture demonstrating tolerance to faults throughout the design and in typically vulnerable voters, using both register transfer level (RTL) and synthesized netlist for fault injection simulation.

## II. BACKGROUND

### A. The `croc` Microcontroller unit

The `croc` MCU design [19] is a simple, open-source<sup>1</sup> SoC. As illustrated in Figure 1a, it features a single 32-bit 2-stage RISC-V core with separate instruction fetch and data interfaces supporting the Open Bus Interface (OBI) protocol. Connected through an OBI interconnect, two static random-access memory (SRAM) banks offer separated data and instruction memory for a total of 16 KiB of memory. The SoC also features a timer module, as well as UART and GPIO peripherals for input/output (IO). Finally, to enable proper programming and basic functionality, the SoC exposes a JTAG interface with a RISC-V debug module, as well as some dedicated control registers for programming and boot.

### B. Fault & Protection Model: Single Events are Corrected

In this paper, we focus on all transient single faults (SEUs & SETs) and the accumulation thereof [20]. Observing at a logic-level, the primary expected effects are SEUs, bit-flips in state-saving elements such as FFs and SRAM bit-cells. The other expected effects are SETs, transient bit-flips in combinational logic, which are less likely to affect the behavior of the design. However, as clock frequencies increase in modern technologies, these are more likely to be captured by FFs [21], [22]. While simultaneous faults are not considered directly, tested SETs may induce multiple faulty SEUs, and SEUs, if not corrected, can accumulate. Furthermore, the design aim is to correct errors and continue operation where possible rather than simply detect faults.

## III. ARCHITECTURE

### A. Fault-tolerant `croc` Architecture

1) *ECC memory*: The first adaptation of the `croc` MCU, described in Section II-A, focuses on the on-chip SRAM. ECC is ideally suited to ensure single faults are correctable

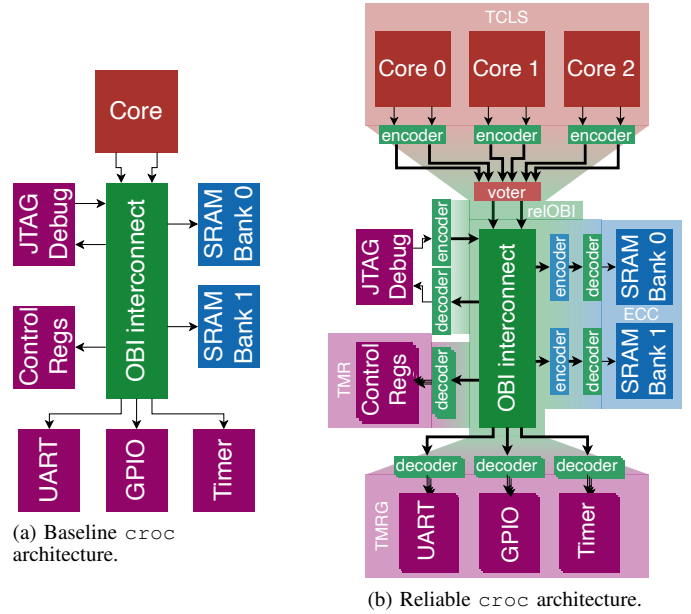


Fig. 1. Block diagram of the `croc` architecture, with (b) showing protected domains highlighted.

without a large area penalty. As such, we ensure each 32-bit word is encoded with 7 additional bits for single error correction, double error detection using a Hsiao code [23]. Each SRAM bank features its own ECC encoder and decoder, with additional logic to support byte-wise writes in a read-modify-write fashion, immediately responding and delaying subsequent accesses for limited performance impact. Furthermore, to ensure errors do not accumulate within the SRAM, a scrubber is added to the design. With a configurable period, it reads all data words in the SRAM, correcting any erroneous words. To avoid impacting performance, it defers its access in case there is an external access to the memory bank. Furthermore, the scrubber also directly corrects any erroneous reads it monitors from external actors.

2) *TCLS core*: The second adaptation focuses on the processor core. Leveraging the work in [12], a static TCLS configuration is implemented for the RISC-V core. The entire processor core is triplicated, with identical inputs connected to the three cores, and voters added for the cores' output bits, most of which are OBI bus signals. In case an error is detected, a software resynchronization routine is executed in an interrupt service routine to ensure any errors remaining within the cores' registers are corrected.

3) *reIOBI interconnect*: The third adaptation focuses on the OBI interconnect between the bus's managers, mainly the processor core, and subordinates, including the SRAM banks and the peripherals. Reliable OBI (reIOBI) [24] augments the OBI protocol with fault tolerance, where critical handshake signals, as well as the interconnection modules' internals, are protected with TMR, ensuring consistency of the transfers and the interconnect state. Data, address, and additional information passed through the interconnect are protected with ECC to avoid excessive area overhead.

4) *TMR peripherals*: The fourth adaptation applies TMR to many of the remaining components in the design. This includes the timer, UART, and GPIO peripherals, which are fully pro-

<sup>1</sup><https://github.com/pulp-platform/croc>

tected using TMRG [7], where we ensure triplicated voters are added after every register to correct any internal latent faults. Furthermore, any memory-mapped registers, such as the SoC control registers, and the corresponding signals and finite state machines, such as the ECC scrubbing unit, are also triplicated. Figure 1 shows all modifications added to the design.

5) *Fault monitoring*: To ensure traceability, faults are monitored and collected in fault counter registers. This enables verification of protection mechanisms both in software and after tapeout. To improve timing, the collected fault signals are pipelined prior to incrementing the counter. Access is ensured to be reliable, but the counter values are unprotected, as they are not part of the operational design.

6) *Remaining components*: Some components in the design are not protected. The debug module, required for bringup and testing, is not designed to be used in an active environment and is thus not hardened. To ensure it does not affect the system, its signals and bus interfaces can be isolated with dedicated units that are protected.

### B. Overlapping protection

Naively combining different fault tolerance methods would result in an implementation where each protection method is considered individually. Investigating a slice of the protected design, Figure 2a shows a processor core protected with TCLS and an ECC-protected SRAM memory. Inserting a reLOBI-protected interconnect in between still leaves parts of this system, the connection between protected regions, vulnerable to faults. Not only are the connections vulnerable, but the voting, encoding, and decoding logic also remain points of failure.

Thus, when combining ECC-protected SRAM and TCLS processor cores with reLOBI, we ensure an overlap of these protection methods to remove any gaps in the protection, as shown in Figure 2b. Instead of voting on raw data, the reLOBI encoders and decoders are integrated within the lockstepped domain, performing the TCLS voting on encoded signals. This ensures that errors in the voters for TCLS are detected and corrected as errors of the reLOBI interface, and that errors in the reLOBI encoding and decoding are detected as TCLS faults, as the units are triplicated with each lockstepped core. Furthermore, as the data encoding in SRAM is identical to the encoding within the reLOBI bus signals, it is directly reused when storing the data to memory, removing the need for additional ECC encoding and decoding at the SRAM bank. Therefore, while any data error in SRAM may be propagated to the reLOBI interconnect, the corresponding decoders will still correct the fault data word, and vice versa.

## IV. EXPERIMENTAL SETUP

To investigate both implementation overheads and fault tolerance benefits, different configurations for the `croc` SoC are investigated, each with incrementally more fault detection and correction methods as outlined above.

- Cfg. 0: No protection / reference
- Cfg. 1: ECC-protected memory
- Cfg. 2: Protected memory & TCLS cores
- Cfg. 3: Protected memory, cores & reLOBI interconnect (with overlap)
- Cfg. 4: Full protection (with overlap)
- TMRG: Related work, explained in Section VI

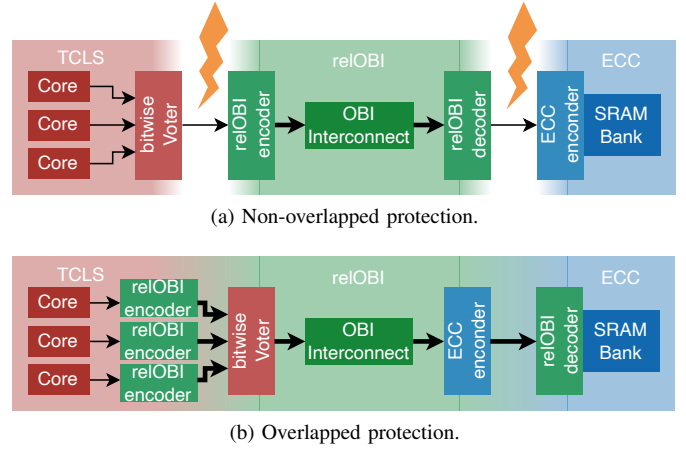


Fig. 2. Section of the design in Figure 1b. Overlapping fault tolerance methods remove vulnerabilities in connecting signals and voting, encoding, and decoding logic in gaps between protected domains.

### A. Implementation Flow

Following the existing setup for the `croc` SoC<sup>1</sup>, the different configurations for `croc` were synthesized with *Yosys* and placed and routed with *OpenROAD* using the open-source IHP 130 nm process design kit with `sg13g2` standard cells at typical conditions. To ensure triplicated elements in the design were not optimized away, hierarchies for these triplicated components or the required fanout and voter cells were kept, ensuring their boundaries and signals are not optimized away. Simple cross-boundary optimizations, such as constant propagation and removal of undriven signals, were allowed, as this does not affect the integrity of the TMR protection.

### B. Fault Analysis

To analyze the `croc` system under faults, we utilize *Synopsys*<sup>®</sup> *VC Z01X™ X-2025.06*, a commercial concurrent fault simulator. Following an initial reference simulation of the `croc` SoC running a particular workload, it concurrently simulates the same design, injecting randomly sampled single faults, tracking the outcome for each simulation.

1) *Workload*: Prior to injecting a fault, the simulation preloads the application into the on-chip SRAM and starts the processor at the corresponding binary location. Thereafter, the core clears the remaining SRAM to ensure there is no faulty data that could indicate an ECC fault. After clearing the fault monitor, the scrubber is started, thereafter allowing the core to enter the main application. This part of the simulation is excluded from fault injection to ensure a reproducible setup, and as this setup process is not expected as part of an operational application loop.

For proper analysis, the tested software is designed to exercise most parts of the SoC, emulating a single loop of a longer application. Thus, the application includes a simple output string transferred over the UART module and toggling of the GPIO pins to verify the IO pins are behaving as expected. A short timer delay is added to ensure the core's interrupts, as well as the timer, are functioning as expected. Finally, a single CoreMark<sup>®</sup> iteration, along with its corresponding check, is executed to ensure the processor performs as expected, storing the number of errors along with a status bit into a return value register to end the application loop.

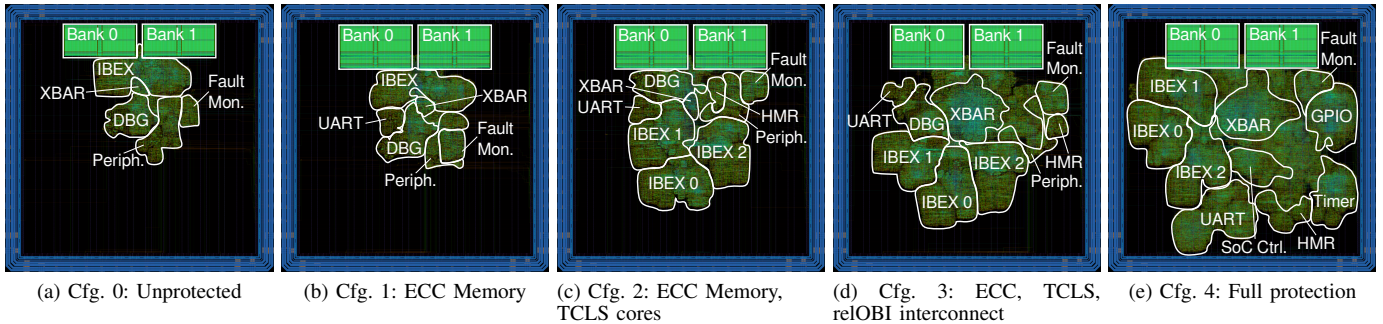


Fig. 3. Annotated implementation layout render for all tested configurations

2) *Monitoring*: To detect the outcome of individual simulations, *VC ZOIX*<sup>™</sup> allows for comparison of individual signals to their values in a reference, non-faulty simulation. By default, we assume a correct outcome with no detected erroneous behavior, which means the injected fault was masked. The SoC’s output pins, the return value register containing the number of errors in the CoreMark<sup>®</sup> calculation, and the core’s exception indicator are compared every cycle. This allows for the detection of any functional issues in the tested SoC components, detected as data errors, processor core exceptions, and timeouts or early terminations.

While some faults may affect the tested iteration loop of the applications, some faults may only become apparent in the following loop iterations or longer-duration applications. As such, at the end of the simulation, we compare the data stored in SRAM to the reference simulation to detect latent faults. These latent faults may be due to a SEU directly in the SRAM that was never overwritten, or due to a corrupted internal state from fault processing that was not otherwise exposed.

Finally, for configurations that contain fault tolerance mechanisms, any correction is logged and differentiated from a simple masked fault outcome. Furthermore, uncorrectable faults, such as multi-bit faults in a single ECC word, are detected and logged as such, irrespective of their correct or incorrect outcome, as we expect a direct triggering of external reset or watchdog logic.

3) *Fault Injection*: For a proper understanding of the behavior of the system under different fault scenarios, 3 sets of experiments are performed, always injecting 100 000 faults for each configuration. The first two experiments emulate SEU faults directly by injecting FF faults into the RTL simulation, flipping the value of a FF or SRAM cell for a single cycle and thereafter allowing the value to be overwritten, much like a SEU affecting a register. While the first scenario targets all possible state bits throughout the SoC, randomly selecting a signal and time point within the active application with equal probability, the second scenario excludes the SRAM from being injected. As the 16kB accounts for over 90% of injectable bits in the design, excluding these allows for more extensive analysis and can help account for differing FF and SRAM cell vulnerabilities.

The third scenario targets the simulation of SETs using the synthesized netlist. To simulate this, we inject PRIM faults, bit-flips in the output of Verilog primitives used to describe the function of the cells in the design, keeping the fault applied across a clock edge to ensure the fault effect

propagates. While this may not model SETs representatively, it ensures the tested faults have a chance to affect the design. As the SRAM is simulated as a behavioral model, it is also excluded from these simulations.

## V. RESULTS

### A. Implementation

All tested *crooc* configurations were synthesized and subsequently implemented on an identical 3×3 mm<sup>2</sup> die at a target frequency of 60 MHz to compare the required area. The placed and routed designs are shown in Figure 3 for all configurations, with more detailed results shown in Table I.

TABLE I  
POST-LAYOUT IMPLEMENTATION RESULTS FOR *crooc* CFGs.

Cfg.	Used Core Area @ 60 MHz	Max. achieved Frequency	Registers	Area Overhead
0	1.057 mm <sup>2</sup> / 146 kGE	112 MHz	5113	1.00 ×
1	1.286 mm <sup>2</sup> / 177 kGE	108 MHz	5254	1.22 ×
2	1.758 mm <sup>2</sup> / 242 kGE	95 MHz	9358	1.66 ×
3	2.171 mm <sup>2</sup> / 299 kGE	65 MHz	10 175	2.05 ×
4	2.867 mm <sup>2</sup> / 395 kGE	62 MHz	13 799	2.71 ×
<i>TMRG</i>	3.676 mm <sup>2</sup> / 507 kGE	70 MHz	11 964	3.48 ×

**Cfg. 0:** The reference design remains fairly compact, as seen in Figure 3a, at 1.057 mm<sup>2</sup> of core area used for cells. While the design can achieve up to 112 MHz clock frequency, a typical target is far lower for this low-performance design. The critical path is shown to originate from the controller in the core’s ID stage, traverse the core’s register file, exit the core through the signals in the instruction fetch interface, negotiate arbitration in the interconnect, and terminate in a register in the core’s load-store unit.

**Cfg. 1:** Adding ECC to the SRAM memory banks increases the total SoC area utilization by around 1.22 ×. While the 7 additional bits for each 32-bit word increase the bits stored by 1.22 ×, the SRAM macros used increase the total utilized SRAM area from 0.528 mm<sup>2</sup> to 0.714 mm<sup>2</sup>, visible in Figure 3b. Along with a 0.043 mm<sup>2</sup> overhead for ECC encoding and decoding, the memory scrubber, and the fault monitoring counters, the area impact remains minimal. The addition of encoding logic affects the maximum achieved frequency, with a similar critical path ending in the SRAM bank after exiting the OBI interconnect arbiter and ECC encoding the data word.

**Cfg. 2:** Tripling the processor cores using TCLS adds 2 additional cores to the design, as well as the required voting

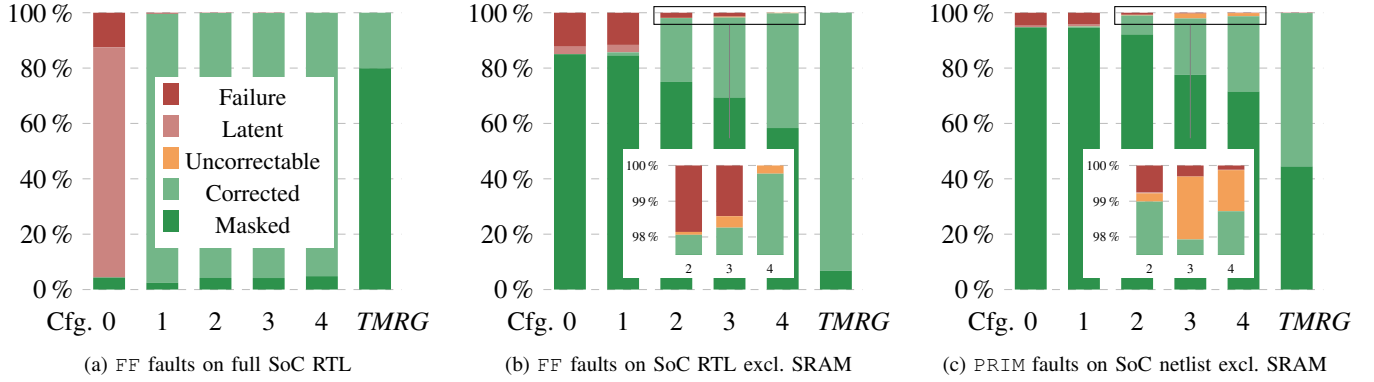


Fig. 4. Fault injection results

and control logic. With each core utilizing  $0.211 \text{ mm}^2$ , an additional  $0.044 \text{ mm}^2$  completes the  $0.472 \text{ mm}^2$  area overhead for the voting logic, configuration registers, and fault monitoring counters, shown in Figure 3c. The voters and corresponding error detection logic add additional timing overhead to the critical path, along with the increasing complexity of the design, making implementation more challenging.

**Cfg. 3:** Adding an overlapping reLOBI interconnect to the SoC adds  $0.413 \text{ mm}^2$  to the total area. This is accompanied by an increased implementation complexity shown in Figure 3d due to the tightly connected triplication of internal modules. Furthermore, due to overlapping, the complexity of other components increases. Triplication also requires more strict module boundary enforcement for implementation, resulting in reduced optimization potential and a more complex design. Furthermore, the additional encoding and subsequent decoding for interconnect signals in reLOBI, such as the address, and triplication results in a significant timing impact, increasing the critical path to support at most 65 MHz. Properly pipelining the fetch interface of the design, as is common in higher-performance systems, and improving the reLOBI architecture to avoid repeated ECC en-/decoding overhead within a single timing path would alleviate the timing penalty.

**Cfg. 4:** Applying fine-grained triplication to the UART, GPIO, and timer modules, as well as all control registers and corresponding logic, results in an additional  $0.696 \text{ mm}^2$  of utilized area. The GPIO module increases from  $0.028 \text{ mm}^2$  to  $0.174 \text{ mm}^2$ , a  $6.2 \times$  area increase, due to the large number of registers and the correspondingly required voters after triplication and their fault detection logic. Similarly, the timer module increases from  $0.028 \text{ mm}^2$  to  $0.150 \text{ mm}^2$ . As the additional components are not on the critical path, only the additional complexity of the design leads to slightly lower maximum frequency.

## B. Fault analysis

All fault-free simulations of the different configurations terminated with identical cycle counts, as the fault tolerance mechanisms do not affect performance in the normal case.

**Cfg. 0:** In the fully unprotected design, 12.54% of injections lead to a failure when injecting FF faults on the entire SoC. As shown in the first bar of Figure 4a, 83.12% of outcomes show correct behavior but still contain latent errors in the SRAM. With over 90% of faults injected into the design being

injected into the SRAM, most of these latent errors simply indicate the flipped bit from injection, but some errors indicate larger impacts on the SoC that can lead to a failure of an application further down the line. Excluding faults in SRAM, we still observe a 12.28% fault rate with 2.70% of simulations resulting in latent errors, shown in Figure 4b. Results for netlist simulations in Figure 4c are lower, showing a 4.70% failure rate and 0.59% latent errors. For both scenarios, excluding SRAM, the latent errors in SRAM are due to SoC errors propagating into SRAM, as the SRAM itself is not injected.

**Cfg. 1:** To address the main source of faults in the complete SoC, we add ECC protection to the SRAM memory banks. This directly addresses all single faults injected into the SRAM, shown in Figure 4a, as a single error in a word is corrected upon reading, either by the system or the scrubber, resulting in a remaining 0.35% failure rate. Errors in the state of the remaining SoC still lead to system failures, with Figures 4b and 4c showing 11.63% of FF faults and 4.31% of faults in the netlist leading to a failure, as well as 2.69% and 0.51% latent errors, respectively. This is similar to the baseline design, as the only protected domain is excluded from these simulations. The slight reduction can be attributed to the additional logic added for encoding and scrubbing, increasing the possible faults, thus reducing the effective fault rate.

**Cfg. 2:** Tackling the largest active component in the design, the processor core, we observe a  $6.2 \times$  and  $5.7 \times$  decrease in failure rates for non-memory registers and netlist faults, respectively, to 1.86% and 0.75%. Studying Figure 4b, we also observe that the number of corrections increases beyond the previous number of failures and latent errors. This is due to both detecting erroneous behavior that may not have led to a failure previously, as well as an increased number of injected faults into the cores, as the random faults are injected evenly distributed across all registers in the SoC. With  $1.8 \times$  more registers as well as correspondingly more logic now in the processor core due to triplication, faults are also more likely to be injected there.

**Cfg. 3:** Adding reliability to the interconnect again reduces the failure rate while increasing the correction rate. With this addition, we observe an increase in the number of uncorrectable errors detected, from 0.08% and 0.23% in Cfg. 2 to 0.32% and 1.77% in Figures 4b and 4c, respectively. Uncorrectable errors indicate multiple-bit errors in a single ECC-protected word, and some are traceable to

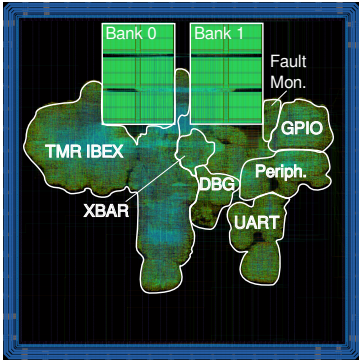


Fig. 5. Annotated *TMRG* layout render

a fault injected in the ECC encoding. Furthermore, faults in the detection or-tree also affect the results.

**Cfg. 4:** The entire active design is now protected, resulting in no detected failure for any injected FF faults in the design. While registers are simpler to ensure they are properly protected, netlist simulations inject faults in primitives, which include both combinational and sequential logic, resulting in a remaining failure rate of 0.12%. These faults can be traced back to components in the design that are not expected to be protected with the available methods, such as the GPIO output signals, which are voted prior to connecting to the single output pad.

While injecting faults into the synthesized netlist provides a good representation of failure rates from the implemented logic, additional transistors, such as clock buffers, are not fully accounted for, but are sure to have a severe impact on the fault tolerance of the design.

### C. Who checks the checker?

To verify the improvement in fault tolerance, we inject PORT faults into the outputs of the TCLS majority voters and the outputs of the ECC decoders in the RTL simulation.

In Cfg. 2, the TCLS majority voters do not overlap with the ECC decoders, located near the SRAM banks. Correspondingly, injecting faults results in 16.33% failures and 1.59% latent errors, with the remaining 82.08% of injected faults being masked.

In Cfg. 3, the ECC decoders are part of the reLOBI protection, which overlaps with the TCLS protection. Therefore, injecting errors in the TCLS majority voters and the reLOBI ECC decoders results in 44.44% of injected faults leading to a correction, and 55.30% of faults masking the injected error. The remaining 0.26% of simulations result in a failure, due to a mismatch in the `core_busy_o` voter output, a signal that is directly monitored as a chip IO but is not otherwise used in the SoC. This highlights that overlapping protection mechanisms even allow for the detection and correction of faults in the encoding, voting, and checking methods themselves.

## VI. RELATED WORK

To compare state-of-the-art (SotA) solutions [2], [6] with our implementation on even ground, we implement `croc` with TMRG [7], triplicating all internal logic protected in Cfg. 4 and adding triplicated voters following every FF. The SRAM banks are triplicated as a whole, and the debug module is excluded from triplication, as in Cfg. 4.

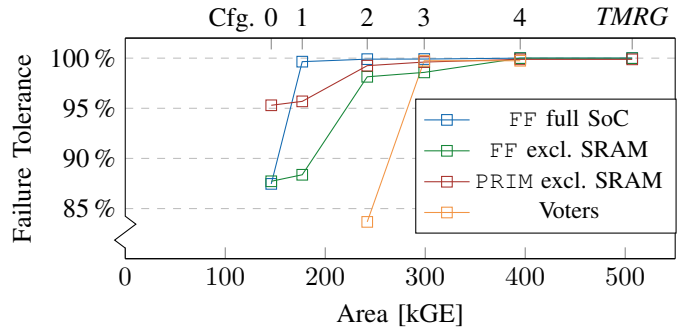


Fig. 6. Pareto-curves of fault-tolerance configurations

The design protected with TMRG exhibits a  $1.28 \times$  higher area overhead than the fully protected design using individual protection mechanisms. While the total number of registers in the design is 13% lower, the additional combinational logic required for fine-grained triplication, and especially the fine interconnections required within, result in a more challenging design to implement and require a larger  $4 \times 4 \text{ mm}^2$  die area, as shown in Figure 5. Timing is also severely impacted due to the increased complexity of the design.

When injecting faults, shown in Figure 4, we see that all SEUs result in a correct outcome, guaranteed by the voting directly after the registers. Latent errors are not measured, but due to the absence of a scrubber, faults in the SRAM banks are not expected to be corrected. Injecting SETs in the synthesized netlist, we observe a 0.12% fault rate. Similar to Cfg. 4, these remaining faults are due to faults in the output voters of IO pins, resulting in incorrect IO behavior.

### A. Pareto Analysis of Design Configurations

To contextualize our results, we define a Pareto frontier as the set of designs for which no lower area alternative configuration provides equal or higher fault tolerance across all fault scenarios. Applying this criterion to our design space, we show in Figure 6 that all of the configurations adding tolerance (Cfgs. 1-4) lie along the Pareto-optimum.

In contrast, fine-grained TMR across the complete design with TMRG lies strictly beyond the Pareto frontier: although it provides almost identical single-fault coverage to Cfg. 4, it requires  $\sim 28\%$  additional area than Cfg. 4 and does not recover the frequency loss, thus offering no dominant improvement.

## VII. CONCLUSION

In summary, we show that individual protection methods can be combined to achieve similar fault-tolerance levels as SotA solutions, such as fine-grained triplication of the entire SoC, with lower area penalties. Properly overlapping the fault-tolerance encodings is crucial to ensure there are no gaps in protection on signals between the fault-tolerant domains or their voting, encoding, or decoding logic. Picking more appropriate methods can greatly improve implementability and reduce the area overhead by 22%.

Incrementally adding different protection methods furthermore allows for requirement balancing, trading off overhead with fault tolerance. Adding ECC-protected SRAM already addresses 97% of failures. Adding fault-tolerance with TCLS for the processor cores addresses 84% of the remaining faults in the design. The final protection methods can achieve fault tolerance on par with SotA at additional cost.

## REFERENCES

- [1] X. Iturbe, D. Keymeulen, P. Yiu, D. Berisford, R. Carlson, K. Hand, and E. Ozer, "On the Use of System-on-Chip Technology in Next-Generation Instruments Avionics for Space Exploration," in *VLSI-SoC: Design for Reliability, Security, and Low Power*, Y. Shin, C. Y. Tsui, J.-J. Kim, K. Choi, and R. Reis, Eds. Cham: Springer International Publishing, 2016, vol. 483, pp. 1–22, series Title: IFIP Advances in Information and Communication Technology. [Online]. Available: [http://link.springer.com/10.1007/978-3-319-46097-0\\_1](http://link.springer.com/10.1007/978-3-319-46097-0_1)
- [2] M. Andorno, A. Caratelli, D. Ceresa, J. Dhaliwal, K. Kloukinas, A. Nookala, and R. Pejasinovic, "Radiation-Tolerant SoC and Application-Specific Processors for On-Detector Programmability and Data Processing in Future High-Energy Physics Experiments," in *2023 12th International Conference on Modern Circuits and Systems Technologies (MOCASST)*, Jun. 2023, pp. 1–5. [Online]. Available: <https://ieeexplore.ieee.org/document/10176589/>
- [3] F. Faubladier and D. Rambaud, "Safety Implications of the use of system-on-chip (SoC) on commercial-of-the-shelf (COTS) devices in airborne critical applications," EUROPEAN AVIATION SAFETY AGENCY, Tech. Rep. EASA\_REP\_RESEA\_2008\_1, Feb. 2008. [Online]. Available: <https://www.easa.europa.eu/en/document-library/research-reports/easarepresa20081#group-downloads>
- [4] O. Ballan, P. Maillard, J. Arver, C. Smith, R. Petersson, A. Griessing, and F. Venini, "Evaluation of ISO 26262 and IEC 61508 metrics for transient faults of a multi-processor system-on-chip through radiation testing," *Microelectronics Reliability*, vol. 107, Apr. 2020.
- [5] J. Andersson, "Gaisler NOEL-V SoC Applications and Ecosystem," ESA ESTEC, Noordwijk, Netherlands, Dec. 2022. [Online]. Available: [http://microelectronics.esa.int/riscv/rvws2022/presentations/06\\_ESA\\_RISC-V\\_in\\_Space-NOEL-V.pdf](http://microelectronics.esa.int/riscv/rvws2022/presentations/06_ESA_RISC-V_in_Space-NOEL-V.pdf)
- [6] A. Walsemann, M. Karagounis, A. Stanitzki, and D. Tutsch, "STRV — a radiation hard RISC-V microprocessor for high-energy physics applications," *Journal of Instrumentation*, vol. 18, no. 02, p. C02032, Feb. 2023. [Online]. Available: <https://iopscience.iop.org/article/10.1088/1748-0221/18/02/C02032>
- [7] S. Kulis, "Single Event Effects mitigation with TMRG tool," *Journal of Instrumentation*, vol. 12, no. 01, pp. C01082–C01082, Jan. 2017. [Online]. Available: <https://iopscience.iop.org/article/10.1088/1748-0221/12/01/C01082>
- [8] X. Iturbe, B. Venu, E. Ozer, J.-L. Poupat, G. Gimenez, and H.-U. Zurek, "The Arm Triple Core Lock-Step (TCLS) Processor," *ACM Transactions on Computer Systems*, vol. 36, no. 3, pp. 1–30, Aug. 2019. [Online]. Available: <https://dl.acm.org/doi/10.1145/3323917>
- [9] M. T. Sim and Y. Zhuang, "A Dual Lockstep Processor System-on-a-Chip for Fast Error Recovery in Safety-Critical Applications," in *IECON 2020 The 46th Annual Conference of the IEEE Industrial Electronics Society*, Oct. 2020, pp. 2231–2238.
- [10] M. Sarraseca, S. Alcaide, F. Fuentes, J. C. Rodriguez, F. Chang, I. Lasfar, R. Canal, F. J. Cazorla, and J. Abella, "SafeLS: An Open Source Implementation of a Lockstep NOEL-V RISC-V Core," in *2023 IEEE 29th International Symposium on On-Line Testing and Robust System Design (IOLTS)*, Jul. 2023, pp. 1–7. [Online]. Available: <https://ieeexplore.ieee.org/document/10224867>
- [11] J. Mach, L. Kohútka, and P. Čičák, "Lockstep Vs Microarchitecture: A Comparison," in *2024 IEEE 37th International System-on-Chip Conference (SOCC)*, Sep. 2024, pp. 1–6. [Online]. Available: <https://ieeexplore.ieee.org/document/10737833/>
- [12] M. Rogenmoser, Y. Tortorella, D. Rossi, F. Conti, and L. Benini, "Hybrid Modular Redundancy: Exploring Modular Redundancy Approaches in RISC-V Multi-core Computing Clusters for Reliable Processing in Space," *ACM Trans. Cyber-Phys. Syst.*, vol. 9, no. 1, pp. 8:1–8:29, Jan. 2025. [Online]. Available: <https://dl.acm.org/doi/10.1145/3635161>
- [13] S. Shukla, Utkarsh, M. Azam, and K. C. Ray, "An Efficient Fault-Tolerant Instruction Decoder for RISC-V Based Dual-Core Soft-Processors," *IEEE Transactions on Circuits and Systems I: Regular Papers*, vol. 70, no. 12, pp. 4816–4825, Dec. 2023. [Online]. Available: <https://ieeexplore.ieee.org/document/10260708/>
- [14] D. A. Santos, A. M. P. Mattos, D. R. Melo, and L. Dilillo, "Enhancing Fault Awareness and Reliability of a Fault-Tolerant RISC-V System-on-Chip," *Electronics*, vol. 12, no. 12, p. 2557, Jan. 2023, number: 12. [Online]. Available: <https://www.mdpi.com/2079-9292/12/12/2557>
- [15] M. Ulbricht, L. Lu, J. Chen, and M. Krstic, "The TETRISC SoC—A resilient quad-core system based on the ResiliCell approach," *Microelectronics Reliability*, vol. 148, p. 115173, Sep. 2023. [Online]. Available: <https://www.sciencedirect.com/science/article/pii/S0026271423002731>
- [16] I. F. V. Oliveira, M. F. Pontes, R. B. Schvitz, L. S. Rosa, P. F. Butzen, and R. I. Soares, "Fault Tolerance Evaluation of Different Majority Voter Designs," in *2022 IEEE International Symposium on Circuits and Systems (ISCAS)*, May 2022, pp. 185–189. [Online]. Available: <https://ieeexplore.ieee.org/abstract/document/9938002>
- [17] M. Rogenmoser, P. Wiese, B. E. Forlin, F. K. Gürkaynak, P. Rech, A. Menicucci, M. Ottavi, and L. Benini, "Trikarenos: Design and Experimental Characterization of a Fault-Tolerant 28-nm RISC-V-Based SoC," *IEEE Transactions on Nuclear Science*, vol. 72, no. 8, pp. 2783–2792, Aug. 2025. [Online]. Available: <https://ieeexplore.ieee.org/document/10978878>
- [18] A. B. de Oliveira, L. A. Tambara, F. Benevenuti, L. A. C. Benites, N. Added, V. A. P. Aguiar, N. H. Medina, M. A. G. Silveira, and F. L. Kastensmidt, "Evaluating Soft Core RISC-V Processor in SRAM-Based FPGA Under Radiation Effects," *IEEE Transactions on Nuclear Science*, vol. 67, no. 7, pp. 1503–1510, Jul. 2020, conference Name: IEEE Transactions on Nuclear Science.
- [19] P. Sauter, T. Benz, P. Scheffler, H. Pochert, L. Wüthrich, M. Povišer, B. Muheim, F. K. Gürkaynak, and L. Benini, "Croc: An End-to-End Open-Source Extensible RISC-V MCU Platform to Democratize Silicon," in *RISC-V Summit Europe*. Paris, France: arXiv, May 2025, arXiv:2502.05090 [cs]. [Online]. Available: <http://arxiv.org/abs/2502.05090>
- [20] P. Dodd and L. Massengill, "Basic mechanisms and modeling of single-event upset in digital microelectronics," *IEEE Transactions on Nuclear Science*, vol. 50, no. 3, pp. 583–602, Jun. 2003. [Online]. Available: <https://ieeexplore.ieee.org/document/1208578/>
- [21] S. Di Mascio, A. Menicucci, E. Gill, G. Furano, and C. Monteleone, "Open-source IP cores for space: A processor-level perspective on soft errors in the RISC-V era," *Computer Science Review*, vol. 39, p. 100349, Feb. 2021. [Online]. Available: <https://linkinghub.elsevier.com/retrieve/pii/S1574013720304494>
- [22] A. Walsemann, M. Karagounis, A. Stanitzki, and D. Tutsch, "Fault tolerance evaluation study of a RISC-V microprocessor for HEP applications," *Journal of Instrumentation*, vol. 19, no. 02, p. C02012, Feb. 2024. [Online]. Available: <https://iopscience.iop.org/article/10.1088/1748-0221/19/02/C02012>
- [23] M. Y. Hsiao, "A Class of Optimal Minimum Odd-weight-column SEC-DED Codes," *IBM Journal of Research and Development*, vol. 14, no. 4, pp. 395–401, Jul. 1970.
- [24] M. Rogenmoser, A. Garofalo, and L. Benini, "reLOBI: A Reliable Low-latency Interconnect for Tightly-Coupled On-chip Communication," in *International Integrated Reliability Workshop (IIRW)*. South Lake Tahoe, CA, USA: arXiv, Oct. 2025, arXiv:2508.05354 [cs]. [Online]. Available: <http://arxiv.org/abs/2508.05354>